Seasonal Predictability of ENSO Teleconnections: The role of the remote ocean response

Hilary Spencer [*†] Julia M. Slingo[2] Mike K. Davey [‡]

December 2003

Abstract

In this modelling study, the teleconnections of ENSO are studied using an atmospheric general circulation model (AGCM), HadAM3. The influence of sea surface temperature anomalies (SSTAs) remote from the tropical Pacific but teleconnected with ENSO is investigated. Composite cycles of El Niño and La Niña SSTs are created and imposed on HadAM3. These SSTs are imposed in different areas, with climatological SSTs elsewhere, in order to find the influences of SSTs in different regions.

It is found that most of the reproducible response to ENSO is forced directly from the tropical Pacific before the peak of the event. However, during the peak and decay of ENSO, remote SSTs become increasingly influential throughout the tropics (at the 98% significance level). This could lead to extended ENSO-related predictability due to the memory of the remote oceans.

The Indian ocean and Maritime Continent SSTs are found to be particularly influential. Indian Ocean SSTAs dampen the teleconnections from the tropical Pacific and force the atmosphere above the tropical Atlantic. More generally, when a tropical SSTA is imposed, atmospheric anomalies are forced locally with anomalies of the opposite sign to the west. Some of the reproducible response to ENSO in the tropical Atlantic is forced, not directly from the tropical Pacific but from the Indian ocean, which in turn is forced by the tropical Pacific. Subsequently, delayed SSTAs in the tropical Atlantic damp the local response and force the atmosphere above the tropical Pacific in the opposite manner.

1 Introduction

The predictable component of atmospheric variability on seasonal timescales is closely associated with SST variability, particularly ENSO (eg. Charney and Shukla, 1981; Brankovic et al., 1994). However, ENSO itself influences SST worldwide (eg. Pan and Oort, 1990) and those influences in turn may impact on seasonal prediction (eg. Lau and Nath, 1994, 1996). Hence it is important to investigate the role of the remote ocean response to ENSO.

Many seasonal forecasts are still produced by coupled ocean/atmosphere models that are only coupled in the tropical Pacific (Latif et al., 1998). These include models with statistical components in the ocean or atmosphere as well as physical components. Some include global ocean models but with only the tropical Pacific SSTs coupled to the atmosphere whereas some include only tropical Pacific ocean models. These types of model are still widely used due to the large systematic errors in fully coupled ocean/atmosphere models (Covey et al., 2000; Latif et al., 2001; Davey et al., 2002) which lead to large errors in seasonal anomalies due to the non-linear dynamics (Molteni and Ferranti, 2000).

There is evidence that atmospheric seasonal predictability is achieved largely by imposing the correct SSTs in the tropical Pacific. For example Lau and Nath (1994, 1996) and Ferranti et al. (1994) have shown with atmospheric global circulation model (AGCM) studies, that tropical Pacific SSTAs are more important than North Pacific SSTAs for reproducing the atmospheric response over the North Pacific and North America. Increasingly, attention is being focussed on the relative influences of the three tropical ocean basins. Kumar and Hoerling (1998) simulated the most realistic response to SSTs with an AGCM when observed SSTs were imposed only in the tropical Pacific with climatological SSTs elsewhere. This was thought to be due to the thermodynamic control of the Indian Ocean by the atmosphere, as well as the influence of the Indian Ocean on the atmosphere, as simulated in an AGCM. However, Goddard and Graham (1999) and Latif et al. (1999) found that the observed Indian Ocean SSTs were important for simulating eastern and southern African rainfall accurately and Hoerling et al. (2001) noted the importance of the Indian ocean SSTAs for North Atlantic climate. AGCM simulations by Barsugli and Sardeshmukh (2002) and Schneider et al. (2003) also showed Indian Ocean SSTAs to be influential on much of the northern hemisphere, Africa and Australia.

It is well known that global SSTs respond in a coherent manner to tropical Pacific SSTs. For example, Pan and Oort (1990) demonstrated the high correlations of global observed SSTs with those in the eastern equatorial Pacific. In particular, they picked out the Indian Ocean with a maximum positive correlation lagged one month behind the eastern equatorial Pacific and the Atlantic ocean lagged three months behind. The mechanisms generating these delayed SSTAs, the "atmospheric bridge", were investigated by Alexander (1992); Lau and Nath (1994, 1996) with AGCM studies and by Klein et al. (1999) studying ship and satellite data. This "atmospheric bridge" was reviewed by

[*] correspondence author, h.spencer@rdg.ac.uk, tel: +44 118 378 6608, fax: +44 118 378 8905
[†] Centre for Global Atmospheric Modelling, Meteorology Department, University of Reading, UK
[‡] Met Office, UK and Dept. of Mathematics, University College London, UK

Alexander et al. (2002), who reported the delays to be between two and six months and the remote SSTAs to be forced predominantly by anomalous surface heat fluxes but to some extend also by anomalous Ekman transport in the central North Pacific.

Other studies have displayed the high correlations of global atmospheric anomalies with tropical Pacific SST and the high simulation skill achieved during strong ENSO forcing (eg. Brankovic et al., 1994; Kumar et al., 1996; Renshaw et al., 1998; Sardeshmukh et al., 2000; Shukla et al., 2000; Graham et al., 2000). However, from these studies it is not known to what extent remote atmospheric anomalies are affected by local SSTAs versus tropical Pacific SSTAs. (Remote in the context of ENSO teleconnections is here taken to mean remote from the tropical Pacific.)

This study focuses on assessing the predictable component of the tropical atmospheric response to ENSO SST forcing and how this response is modified by ENSO-associated feedbacks remote from the tropical Pacific. The skill of seasonal forecast systems depends in part on their ability to represent these remote ENSO-associated feedbacks, so an improved understanding of the remote effects may lead to advances in long range forecast skill.

Seasonal predictability depends on the reproducibility of the atmospheric response, the predictability of the ocean and land surface and the accuracy of the atmospheric model. Spencer and Slingo (2003) studied the accuracy of the modelled atmospheric response to observed ENSO SSTs by the AGCM, HadAM3, used in this study, and found that large scale fields such as sea level pressure and upper level circulation are well simulated in the tropics in December to February (DJF), although the details of the tropical response, especially over land, and the extratropical responses were not so accurate.

In this study we are not addressing the ocean and land surface predictability. Instead, HadAM3 is being used as a perfect model to study the reproducibility of the large scale tropical response to ENSO SSTs. The relative importance of tropical Pacific and remote ENSO SSTs in forcing the atmosphere during and after a strong ENSO event is investigated. It is important to study the demise of the events if extended predictability is sought since there may be possibilities for extended predictability due to the memory of the ocean and land.

In order to study the effects of remote SSTAs teleconnected with ENSO (remote ENSO SSTAs) on the global response to ENSO, SST composites are created for cycles of both events. These composites are then imposed as the lower boundary condition to an AGCM. Creation of the composite from a large number of events reduces the influence of large coincident remote SSTAs disconnected with ENSO. This compositing technique and the experimental design and validation are described in section 2, along with the definition of the different experiments with SSTAs imposed in different areas. Section 3 describes the results of the different experiments with emphasis on DJF at the peak of El Niño and the following JJA. The results are discussed further and final conclusions are drawn in section 4.

2 Experimental Design

The purpose of this experiment is to study the influence on the atmosphere of SSTAs remote from the tropical Pacific but teleconnected with ENSO (remote ENSO SSTAs). These SSTAs can either damp or enhance the immediate response and may extend local responses after the tropical Pacific forcing has decayed or they may influence the atmosphere remote from the SSTA. To this end, a range of AGCM experiments with HadAM3 is performed with SSTs imposed evolving between typical El Niño and La Niña states and each including different aspects of the global ENSO SSTs.

It is difficult to do such a clean experiment with SSTs from observed events because all events are different and each event is accompanied by different combinations of unrelated phenomena around the globe. For example, although ENSO may influence the North Atlantic region, the effects of ENSO in this region cannot be studied by looking at a few observed events. Other modes of variability, internal to the Atlantic, may dominate the signal. To illustrate, the SSTAs of two El Niño events in DJF of 1957/58 and 1972/73 are shown in figure 1 taken from the GISST dataset (version 2.3b, Parker et al., 1995). For these two events, the SSTAs in the tropical Pacific are similar but the SSTAs elsewhere are very different in places, particularly in the Atlantic.

As well as different El Niño and La Niña events coinciding with different phenomena elsewhere around the world, the timing of events within the seasonal cycle can be different, making the atmospheric teleconnections dependent on the season as well as on the phase of the ENSO cycle. The variation between events in terms of the timing, duration and size is well illustrated by the Niño 3 index, the SSTA in the Niño 3 area, 5°S- 5°N and 90°W - 150°W (The Niño 3 area is shown in figure 1 and the index time series in figure 2).

2.1 Composite El Niño and La Niña SST fields

Composite SST fields are created from the monthly GISST dataset (version 2.3b, Parker et al., 1995) from 1870 to 1998. In order to reduce high frequency variability not associated with ENSO, a "14641" binomial filter by month is applied:

$$\bar{T}_i = \frac{1}{16}T_{i-2} + \frac{4}{16}T_{i-1} + \frac{6}{16}T_i + \frac{4}{16}T_{i+1} + \frac{1}{16}T_{i+2} \quad (1)$$

where T_i is the monthly mean value of SST at each grid point and $\bar{T}_i$ is the filtered value for month i.

The composite SST fields are constructed based on the January Niño 3 index. January is chosen as the base month since it is close to the peak of many ENSO cycles. Each January is included in either the El Niño or La Niña composite if its Niño 3 index is greater than the mean positive January Niño 3 index (0.80°C) or less

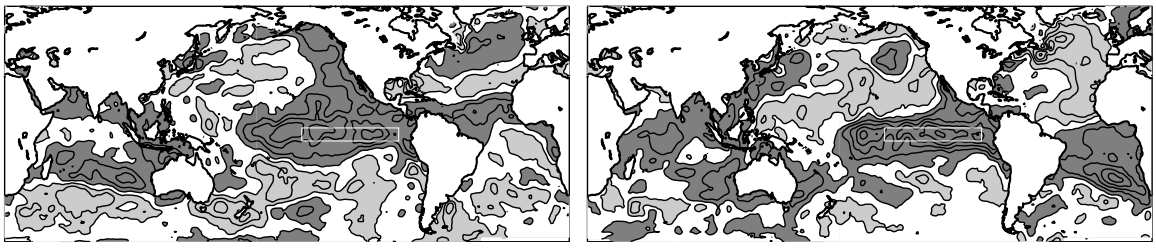

1957/58 1972/73

Figure 1: The SSTAs of two El Niños in DJF from the GISST dataset (version 2.3b, Parker et al., 1995). (Niño 3 area marked) The contour interval is 0.4°C. Positive anomalies have dark shading and negative anomalies, light shading

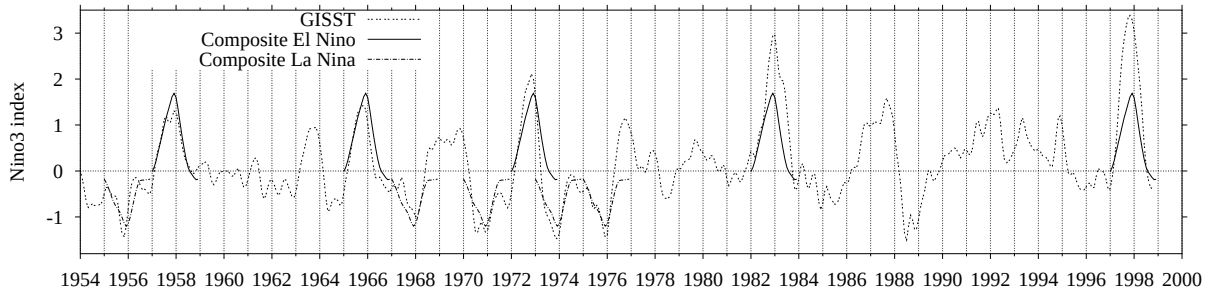

Figure 2: The Niño 3 index from the GISST dataset compared with composites of many El Niños and many La Niñas. The dataset has been passed through a "14641" binomial filter by month. (The anomaly is calculated from the 1870 to 1998 climatology)

than the mean negative January index (-0.6°C) respectively. The mean positive and mean negative Niño 3 index values are used to diagnose El Niño and La Niña rather than the standard deviation (0.88°C) since the distribution of the Niño 3 index is skewed and El Niño events tend to be bigger and less frequent than La Niña events. In order to avoid a sharp cutoff, and because there is no distinct threshold for ENSO events, cases are also included if their indices are close to these critical values but are given smaller weights. The weights given to different fields for the El Niño composite are calculated using a Gaussian function to join the weights of zero and one (a smoothed Heavyside function):

$$weight = \begin{cases} 0 & \text{for } N3 < \frac{1}{2}\mu^+ \\ \exp\left\{-\left(\frac{\mu^+ - N3}{\frac{\mu^+}{4}}\right)^2\right\} & \text{for } \frac{1}{2}\mu^+ \leq N3 \leq \mu^+ \\ 1 & \text{for } N3 > \mu^+ \end{cases} \quad (2)$$

where μ^+ is the mean positive Niño 3 index for January and $N3$ is the Niño 3 index. The weights for the La Niña composite are calculated similarly. Various changes to this compositing technique have been tried with only small differences to the results.

The resulting composite SSTAs for January El Niño and La Niña are shown in figure 3. These have been scaled by a factor of 1.32 to make the Niño 3 index of the January El Niño exactly twice the mean positive Niño 3 index. This choice of a Niño 3 index is arbitrary but this size of anomaly field is considered sufficient to force HadAM3 significantly and is considered to be typical for a large event. Also shown in figure 3 are the different areas over which ENSO SSTA are imposed in the different experiments.

2.2 Two year El Niño and La Niña composites

The definition of the composites for El Niño and La Niña in January is given above. However a cycle is required that includes the evolution of both events. Therefore lead and lag composites are created for the 12 months leading up to and following on from all the Januaries included in the composites. The same weighting factors for the leading and lagging months are used. This procedure gives a 24 month El Niño composite and a 24 month La Niña composite. At the end points of these composites, the SST has returned to similar weak La Niña conditions so the two events can be concatenated to create a four year ENSO cycle. The resulting El Niño and La Niña composites of the Niño 3 index are plotted in figure 2 over a number of significant observed events.

As example months in the composite, the July before and after the peak of the El Niño composite are also shown in figure 3. The July before the peak shows the strong warming in the tropical Pacific and a horseshoe of colder water in the western tropical Pacific due to the coupled ocean/atmospheric dynamics local to this area. However, the remote ENSO SSTAs are still weak. In January at the peak of the event, there are large areas of warming across the Indian ocean and some in the tropical Atlantic. There are also regions of warm and cold water extending poleward across the Pacific which are manifestations of the extratropical atmospheric Rossby wave response to El Niño.

Six months after the peak of the event, in July, the

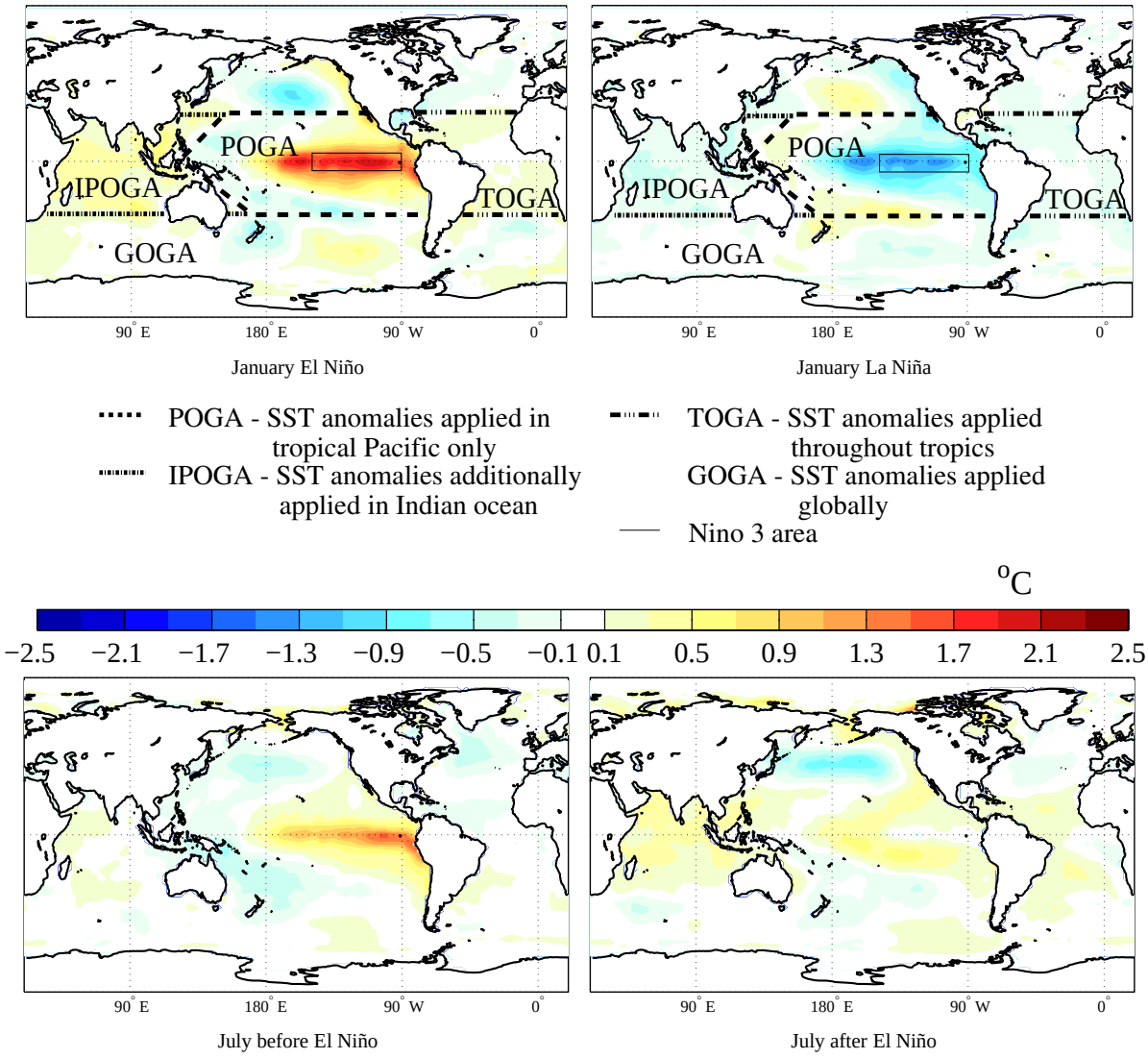

Figure 3: SSTAs of the composite ENSO events scaled by 1.32 and the areas SST applied over for the different experiments

Indian Ocean warming and the North Pacific cooling have decayed slightly but the tropical Atlantic warming has increased further. In contrast, the tropical Pacific SSTAs have decayed almost completely and a swing towards La Niña is in progress.

2.3 Experiment Definitions

In section 2.2, a 48 month composite was described consisting of a 24 month growing and decaying El Niño followed by a 24 month growing and decaying La Niña. In order to create lower boundary conditions for 40-year AGCM integrations, ten such cycles are concatenated, the Niño 3 index of the resulting SST field is shown in figure 4. This is the SST field which is applied as a lower boundary condition to the ENSO experiments. The ENSO cycle is repeated ten times to achieve significant results.

In order to estimate the importance of the remote ENSO SSTAs in comparison with tropical Pacific SSTAs, a series of experiments are run with different SSTs imposed in different areas. The first experiment has the ENSO composite cycle of SSTs defined above applied only in the tropical Pacific with the climatological seasonal cycle of SSTs applied elsewhere. This is denoted the “POGA” experiment for “Pacific Ocean, Global Atmosphere” (see figure 3). To avoid discontinuities in SST on the northern and southern boundaries, a linear interpolation between the Pacific ENSO and climatological SSTs is applied between 24° and 30° latitude. The western boundary is chosen to be where the SSTAs are approximately zero. This area contains the primary SSTAs associated with ENSO, as opposed to the remote ENSO SSTAs whose influence is under study.

The second experiment has the ENSO composite cycle of SSTs imposed globally. This is denoted “GOGA” for “Global Ocean, Global Atmosphere”. In order to understand the relative contributions of the tropical Indian and Atlantic ocean ENSO SSTAs, two further experiments have been performed. The third

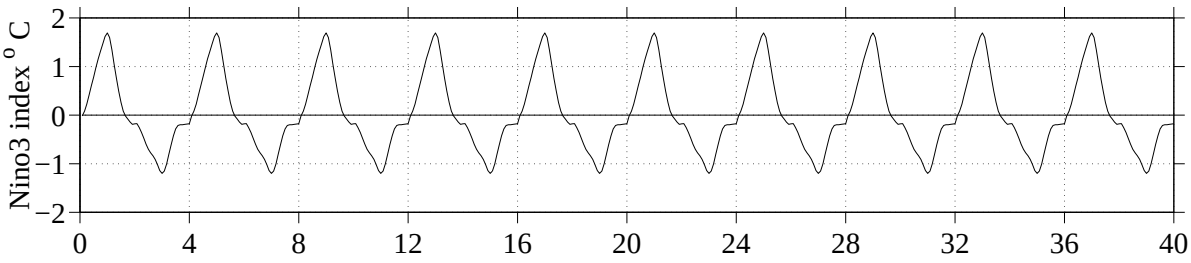

Figure 4: The Niño 3 index of the 24 month El Niño composite and the 24 month La Niña composite concatenated and repeated

experiment is run applying the ENSO SSTs in the entire tropical Pacific and Indian Oceans with climatological SSTs elsewhere. This experiment is denoted "IPOGA" for "Indian and Pacific Ocean, Global Atmosphere" and again the geographical extents of the SSTs applied are shown in figure 3. Finally, in order to confirm which part of the signal is emanating from the tropical Atlantic and which from the extratropics, the fourth experiment has ENSO SSTs imposed throughout the tropics with climatological SSTs elsewhere. This is denoted "TOGA" for "Tropical Ocean, Global Atmosphere". Again the SSTs are linearly interpolated from 24° and 30° between the ENSO SSTs and the climatological SSTs.

On seasonal timescales, the forced atmospheric response is usually assumed to be in equilibrium with the SST forcing (eg Schneider et al., 2003; Alexander et al., 2002) and therefore the time dependence of the SSTAs is not relevant. However, there may be lagged atmospheric response to, for example, snow depth or soil moisture anomalies which may have longer memory than the atmosphere (eg. Fennessy and Shukla, 1999; Koster et al., 2001; Becker et al., 2001). These experiments have been designed with realistic, evolving SSTAs so that these delayed responses are included. However, due to uncertainties in model accuracy, the influences of soil moisture and snow depth anomalies are not studied specifically in this paper.

2.4 The Atmospheric General Circulation Model, HadAM3

The HadAM3 AGCM is described by Pope et al. (2000) and is found to reproduce the observed mean climate well. The standard climate version of the model has a horizontal grid of 2.5° latitude by 3.75° longitude and 19 vertical levels. The model is hydrostatic and uses the Arakawa B grid and Eulerian advection. Moist and dry convection are parameterised with a mass flux scheme (Gregory and Rowntree, 1990) and clouds only form in grid boxes with relative humidity greater than a critical value of 70%.

Spencer and Slingo (2003) performed a detailed diagnosis of the accuracy of the atmospheric response in HadAM3 to ENSO SSTs. They found that the response of large scale fields such as sea level pressure and stream function in DJF at the peak of El Niño is fairly realistic in the tropics. However, the extratropical response is not so well captured due to small but significant differences in the tropical Pacific precipitation response. Therefore, this study will focus primarily on the tropical response to El Niño. Some improvement was found in the details in the tropical Pacific response and in the extratropics using 30 vertical model levels instead of 19. Therefore some of the experiments described here are repeated with the version of the model with 30 vertical levels.

2.5 Validation of ENSO experiment

For the results of these experiments to be useful, two types of validation need to be done. First, the accuracy of the response of HadAM3 to ENSO SST forcing needs to be validated (see Spencer and Slingo (2003)) and secondly, the realism of the experiments described here must be demonstrated, $i.e.$ it must be shown that the composite El Niño and La Niña represent realistic events and that the model responds in a realistic way to these SSTs.

In order to demonstrate the realism of these experiments, the sea level pressure anomalies in DJF at the peak of El Niño and for the following JJA from the "GOGA" experiment with 19 and 30 vertical model levels are shown in figure 5. These are compared with a composite of five El Niño events from an ensemble of six integrations of HadAM3 with 19 vertical levels and with observed SSTs. This composite of five El Niño events is described by Spencer and Slingo (2003). Since the idealised composite El Niño has a Niño 3 index of 1.6°C in January and the composite of five has a Niño 3 index of 2°C, the sea level pressure anomaly composites of five are scaled by 0.8 so that they are more comparable with the results with the idealised ENSO SSTs imposed. The comparison between "GOGA" with 19 levels and the HadAM3 ensemble with observed SSTs does not yield identical results due to the internal variability in the model and the different SSTs imposed, but the large scale responses in the tropics are very similar in DJF. In order to demonstrate the accuracy of the model, a comparison is also made with the NCEP reanalysis (Kalnay et al., 1996) for the same events. Again, the large scale responses in the tropics are similar in DJF. Systematic model errors of the extratropical teleconnections are discussed by Spencer and Slingo

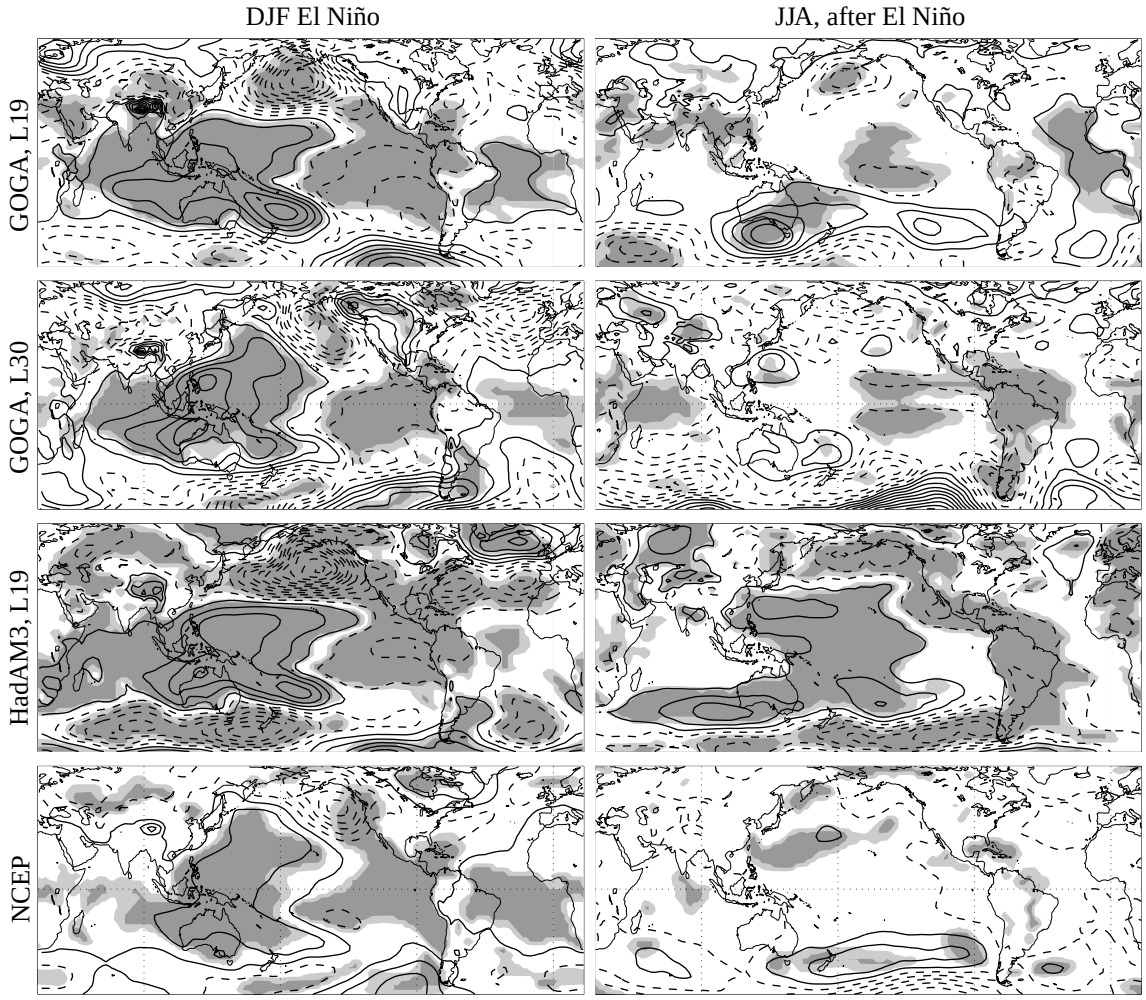

Figure 5: Mean sea level pressure anomalies for the "GOGA" experiment El Niño years (for HadAM3 with 19 and 30 vertical levels), a composite of El Niño years 1957/58, 1965/66, 1972/73, 1982/83, 1997/98 from the HadAM3 ensemble with observed SSTs and the NCEP reanalysis data. The contour interval is 0.5hPa and negative contours are dashed and start at -0.25hPa. Values significantly different from zero at the 98% level are darkly shaded and at 95% level lightly shaded. The HadAM3 and NCEP composites of observed years are scaled by 0.79 so that the Niño 3 SSTA is 1.6°C as in the experiments

(2003).

The results of the "GOGA" experiments with 19 and 30 model levels are not identical in the tropics. However, the "POGA" experiment was also run with 30 vertical levels (not shown) and, importantly, the differences between "GOGA" and "POGA" with 19 levels are similar to the differences between "GOGA" and "POGA" with 30 levels in the tropics. Therefore the enhanced vertical resolution does not affect the influences of the remote ENSO SSTAs and the other experiments are run with 19 vertical levels.

The similarity between "GOGA" and the HadAM3 ensemble in JJA is less marked mainly because there are large differences in the SSTAs imposed. The accuracy of the model in JJA following El Niño is assessed by comparing the HadAM3 ensemble composite with the NCEP composite. Again the weak tropical anomalies are coincident with more significant anomalies in the HadAM3 ensemble as expected. The North and South Pacific are also well simulated.

The comparison between the HadAM3 ensemble with observed SSTs and the NCEP reanalysis in figure 5 confirms the realistic tropical response in DJF and JJA. It also shows the lack of significant anomalies in the NCEP data in JJA which highlights the need for ensemble integrations and experiments such as these.

3 The Results of the ENSO Experiments

3.1 Sea Level Pressure

3.1.1 El Niño

The sea level pressure anomalies averaged over the ten El Niños of each of the experiments in DJF and JJA after the peak of El Niño are shown in figure 6. For "POGA", values significantly different from zero at the 95% and 98% confidence levels based on a t-test are light and dark shaded respectively. For the other experiments, the areas significantly different from "POGA" at the 95% and 98% levels are shaded.

Low pressure anomalies in the central and eastern tropical pacific in "POGA", a local response to the

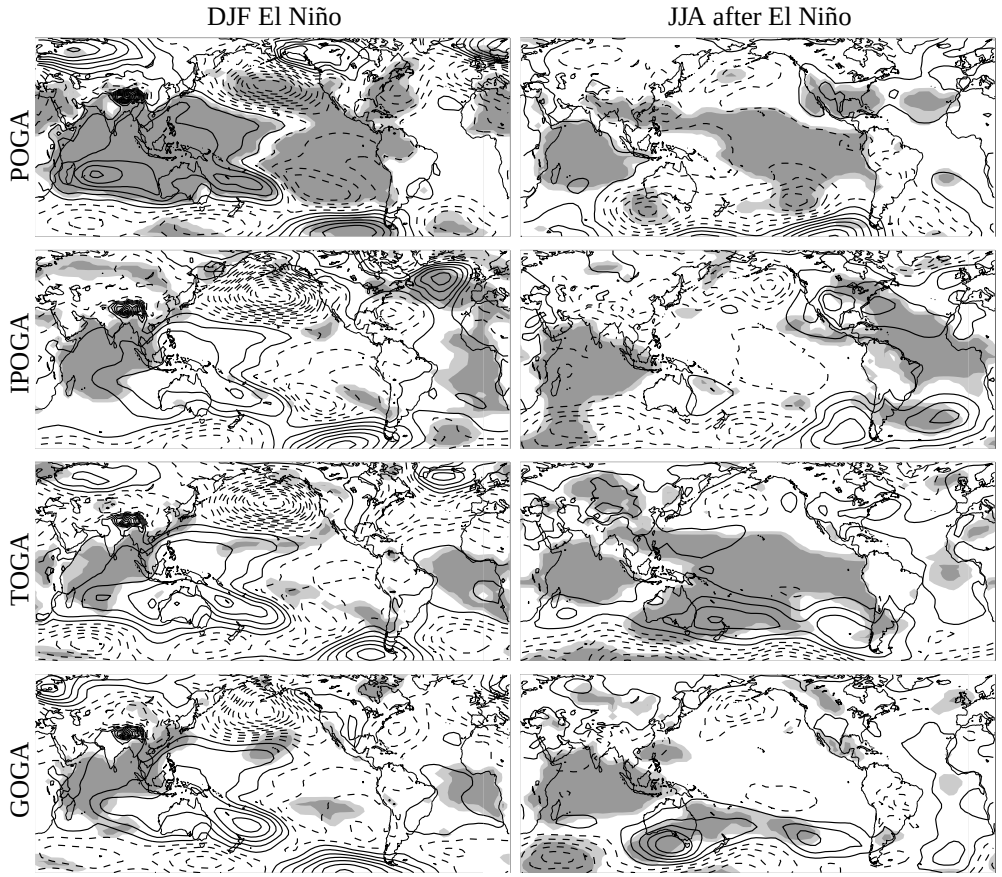

Figure 6: El Niño composite mean sea level pressure anomalies for the ENSO experiments The contour interval is 0.5hPa, negative contours are dashed and start at -0.25hPa. For "POGA", values significantly different from zero at the 98% and 95% confidence level are shaded dark and light respectively. For the other experiments, values significantly different from "POGA" at the 98% and 95% confidence level are shaded dark and light respectively.

warm SSTAs, are balanced by high pressure over the West Pacific and Indian oceans; in other words there is a westwards shift of mass, the well known Southern Oscillation. Is should be noted that this strong response over the Indian Ocean is not similar to that observed, as shown in figure 5, whereas the "GOGA" response in DJF is more realistic. This is contrary to the results of Kumar and Hoerling (1998) whose simulation degraded on the inclusion of observed Indian Ocean SSTs. This was thought to be due to the fact that warm SSTAs in the Indian Ocean force convection in an AGCM whereas, additionally, clear skies create warm SSTAs in the Indian Ocean in reality. However, it was acknowledged that systematic model errors would also influence their results. Indeed, the fact that the simulation is improved in "GOGA" in comparison to "POGA" in these experiments indicates that HadAM3 has a more realistic response to Indian Ocean SSTAs in comparison to tropical Pacific SSTAs.

When the warm SSTAs, part of the remote response to ENSO, are imposed in the Indian ocean and Maritime Continent in "GOGA", "IPOGA" and "TOGA", the large high pressure anomaly in the south west of the Indian ocean is damped and weak high pressure is forced in the tropical Atlantic. This high pressure over the tropical Atlantic could not have been forced locally because cold SSTAs have not been imposed here for more than six months. Therefore it must be a teleconnection. However, it cannot be a teleconnection directly from the tropical Pacific as it is not present in "POGA". Therefore, either the Indian or the extratropical oceans are influencing the tropical Atlantic in DJF. This high pressure over the tropical Atlantic is stronger in the "IPOGA" experiment but of similar magnitude to "GOGA" in the "TOGA" experiment. This leads to the conclusion that the high pressure over the tropical Atlantic is forced by the warm SSTAs in the Indian Ocean and then damped by the local warm SSTAs in the tropical Atlantic. Again there is a westwards shift of mass due to the warm SSTAs, this time in the Indian ocean.

In JJA, after the peak of El Niño, the differences between the experiments are more substantial. This is expected because the tropical Pacific SSTAs have decayed in comparison to the remote ENSO SSTAs. In "POGA", the high pressure anomaly over the Indian ocean persists but there are still no high pressure anomalies in the tropical Atlantic unlike all the other experiments. "IPOGA" has the strongest tropical Atlantic high pressure anomalies since it does not have tropical Atlantic warm SSTAs to damp this high pressure. There are also now differences in the tropical Pacific between the experiments. In particular, "TOGA", which has trop-

ical Atlantic warm SSTAs, now shows higher pressure in JJA over the tropical Pacific than "POGA" and "IPOGA". However this influence, from the Atlantic to the tropical Pacific, is not significant in "GOGA". It has therefore been obscured by influences from the extratropical SSTAs imposed.

A more general conclusion from these results is that the tropical ocean basins force the atmosphere directly above them and the atmosphere above the ocean basin to the west in the opposite manner. Subsequently, the forcing of the atmosphere above the ocean basin to the west is damped by the SSTAs of that ocean basin. The other conclusion is that the results are very different throughout the tropics in this atmosphere-only model in JJA after El Niño when forced by the tropical Pacific only rather than by the entire tropical oceans. This indicates that accurate modelling of remote ENSO-associated SSTAs should improve longer lead time seasonal forecasts, by capturing the influences of the delayed response to El Niño.

3.1.2 La Niña

The sea level pressure anomalies averaged over the ten La Niñas of each of the experiments in DJF and JJA after the peak are shown in figure 7. The large scale response in the tropics is very similar but opposite to that for El Niño. The tropical Pacific SST forces its local atmosphere, with opposite anomalies to the west over the West Pacific and Indian ocean in "POGA". Once Indian ocean SSTAs are included in the other experiments, the Indian ocean response is damped and shifted to the tropical Atlantic. Again, it appears to be the Indian ocean forcing the atmosphere above the Atlantic rather than the tropical Pacific directly. The La Niña results and the differences between the experiments are generally weaker than those for El Niño which is to be expected since the SST forcing is weaker (figure 4).

3.1.3 Area Average Time Series

In order to summarise the sea level pressure results over the tropical Indian and Atlantic oceans for all seasons of El Niño and La Niña, time series of area averages are plotted for each experiment. The Indian ocean (60°E to 120°E and 25°S to 25°N) and tropical Atlantic (40°W to 0° and 25°S to 25°N) sea level pressure area averages are plotted in figure 8 along with the Niño 3 index. The time series have been band pass filtered with a Lanczos filter with a cut-off frequency of 6 months. This cut-off frequency entirely removes seasonal and intraseasonal variability and hence highlights the ENSO variability. In both regions, "TOGA" and "GOGA" give similar results, indicating the dominance of the influence of the tropical SSTs. Above the Indian ocean, "POGA" gives a much larger response throughout both events. However, this response is damped once Indian ocean SSTAs are imposed in "IPOGA" which then gives similar results to "GOGA" and "TOGA" in this region.

Over the tropical Atlantic, "IPOGA" gives a much larger response after the peak of both events and "POGA" gives a weaker response during and after El Niño. This implies that the atmosphere above the Atlantic ocean is being forced by the SSTAs imposed in the Indian ocean and this forcing is damped if local, tropical Atlantic SSTAs are imposed.

3.1.4 Reproducibility of the tropical anomalies

Taylor diagrams (Taylor, 2001) are a convenient way of displaying comparison statistics. They are plots in polar co-ordinates with normalised standard deviation in the radial direction and pattern correlation in the axial direction. They are usually used to compare models with observations but here they are used to compare the ENSO experiment composites with one member of the "GOGA" experiment. (Thus each "GOGA" member in turn represents the observation.) This will show how reproducible the tropical response of "GOGA" is and how much of the response can be reproduced by other experiments.

For "GOGA", the pattern correlation value for a particular season is calculated by first calculating the correlation of "GOGA" member j with the composite of "GOGA" without member j, then averaging over each members j. For other experiments, denoted "xOGA", the pattern correlation is calculated by first calculating the correlation of "GOGA" member j with the composite of "xOGA" without member j and then averaging over each member j. Results are displayed in figure 9 for each season of El Niño and La Niña. The radial direction represents the standard deviation of the tropical sea level pressure field for one member of "GOGA" divided by the standard deviation for each experiment composite. Therefore, for the "GOGA" composite, this represents the signal to noise ratio and for the other experiments it represents the over all magnitude of the reproducible tropical response in comparison to the "GOGA" response. An experiment composite that is identical to every "GOGA" member will be at (1,1) and the distance from (1,1) is a measure of the skill of that experiment at reproducing the "GOGA" response. Therefore, experiments are only significantly different from "GOGA" if they are significantly further from (1,1) than the "GOGA" response is from (1,1) for that season.

The tropics wide Taylor diagrams for El Niño show that, between JJA0 and MAM1 (seasons 2 and 5), the "GOGA" response is highly reproducible, with pattern correlations of almost 0.8 and a signal to noise ratio of between 0.8 and 1. In JJA1 (season 6), the pattern correlation and signal to noise ratio both fall to around 0.4 between each "GOGA" event and the "GOGA" composite meaning that much less of the tropical response is reproducible.

Between JJA0 and MAM1 (seasons 2 and 5) of El Niño, much of the reproducible "GOGA" response is captured by the other experiments meaning that much of the reproducible response is forced by the tropical Pacific. From SON0 (season 3) onwards, the "POGA"

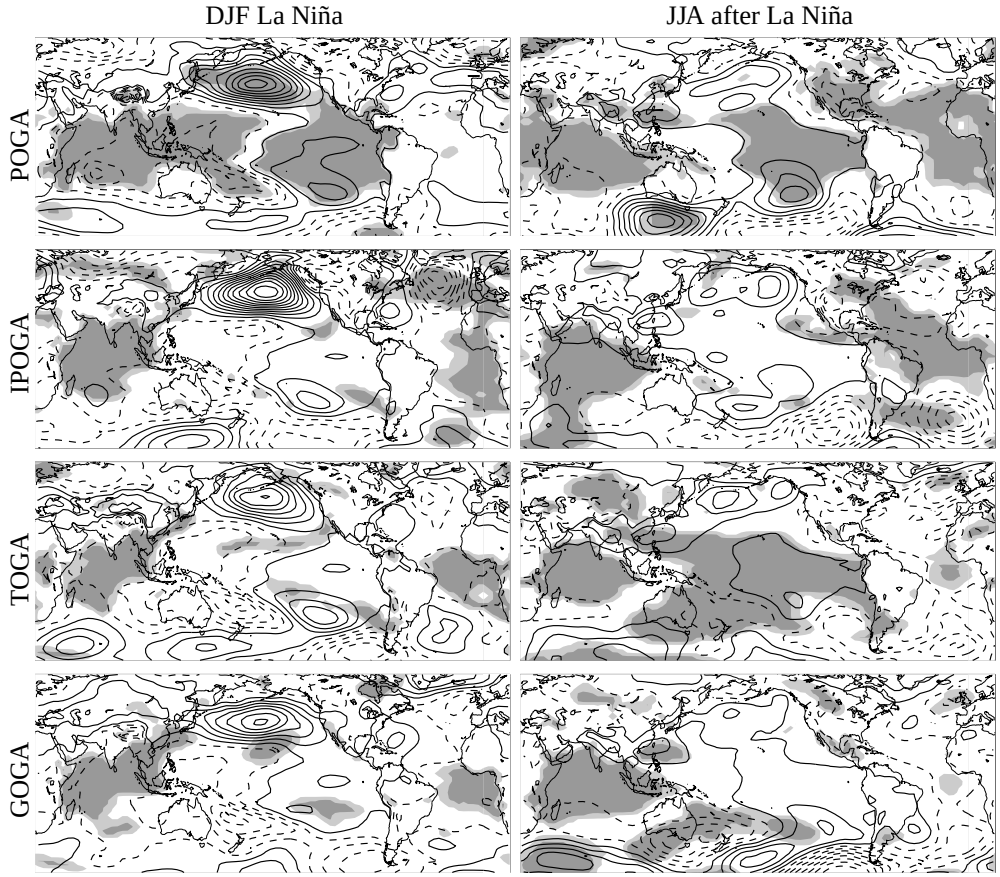

Figure 7: La Niña composite mean sea level pressure anomalies for the ENSO experiments The contour interval is 0.5hPa, negative contours are dashed and start at -0.25hPa. For "POGA", values significantly different from zero at the 98% and 95% confidence level are shaded dark and light respectively. For the other experiments, values significantly different from "POGA" at the 98% and 95% confidence level are shaded dark and light respectively.

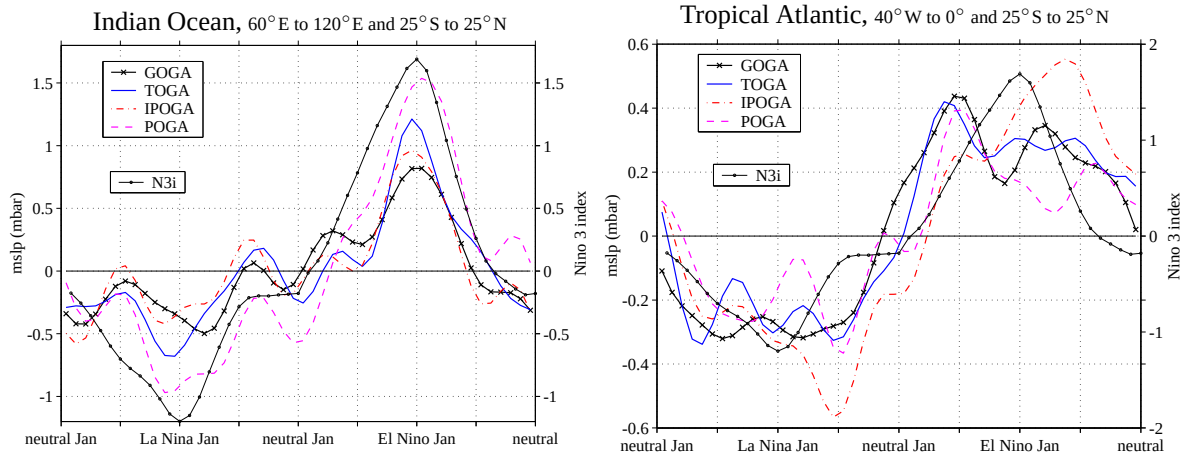

Figure 8: Composite time series of area averaged sea level pressure for La Niña followed by El Niño of each ENSO experiment. Low pass Lanczos filtered with cut-off frequency of 6 months

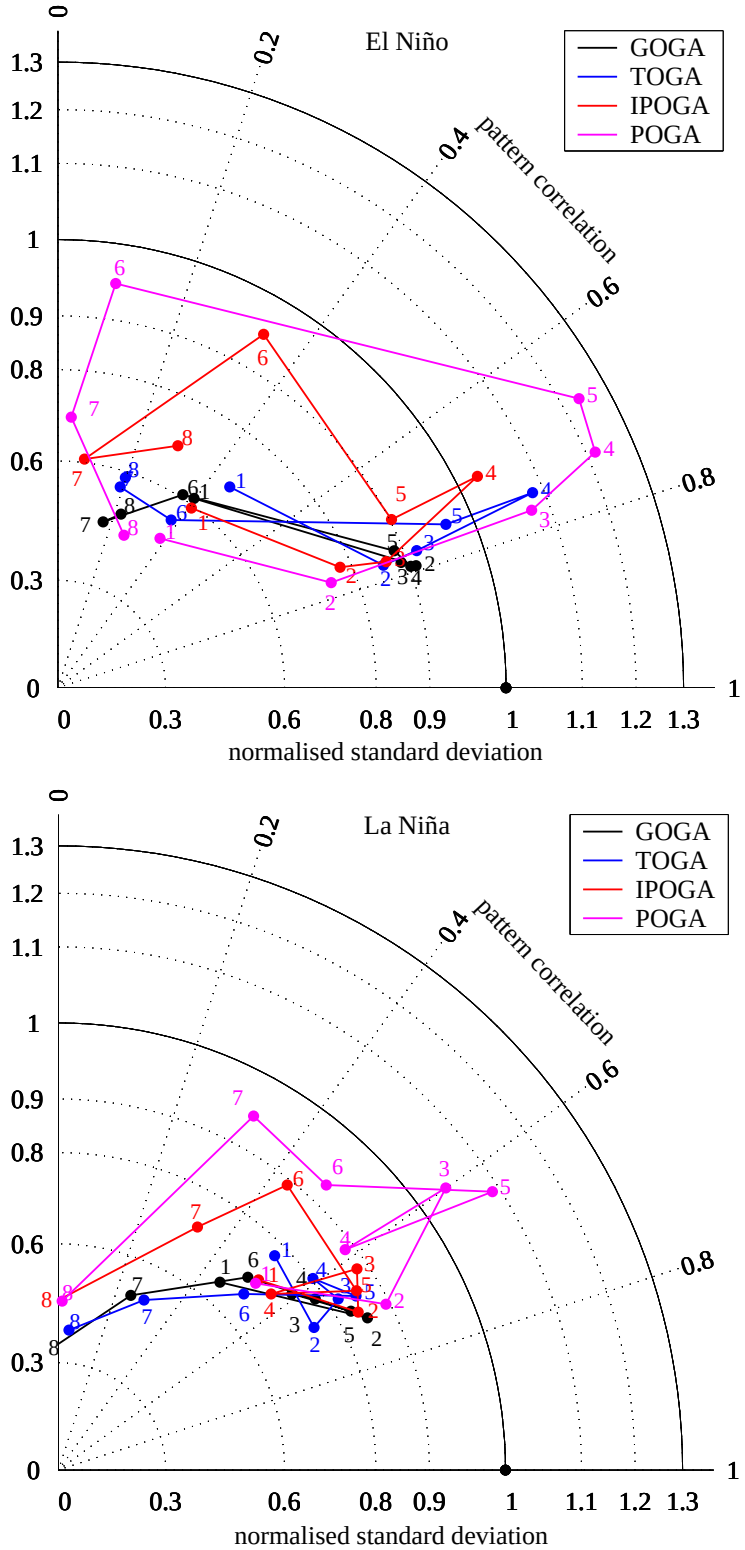

Figure 9: Taylor (2001) diagrams of sea level pressure anomalies throughout the tropics (30°S to 30°N) between each experiment composite and individual events of "GOGA".

1=MAM0, 2=JJA0, 3=SON0, 4=DJF0, 5=MAM1, 6=JJA1, 7=SON1, 8=DJF1

response is too strong due to the lack of damping by remote ENSO SSTAs. In JJA1 (season 6) after El Niño, the "POGA" and "IPOGA" pattern correlations are significantly lower than the pattern correlations for "GOGA" and "TOGA", indicating the importance of the Indian and tropical Atlantic oceans for achieving the small amount of reproducibility after El Niño. (The significance of this pattern correlation is based on the size of the distance between, for example, the "POGA" point 6 and (1,1) in comparison to the distance between the "GOGA" point 6 and (1,1).)

During La Niña, the remote ENSO SSTAs have less of an influence on the pattern correlations. However, around the peak of the event, again the "POGA" response is too strong as there is no damping by remote ENSO SSTAs. Again, during the decay of the event, the "IPOGA" pattern correlations are significantly lower than those for "GOGA" and "TOGA" indicating the importance of the tropical Atlantic during the decay phase. However, the "IPOGA" pattern correlation is significantly higher than that for "POGA" due to the continuing importance of the Indian ocean.

3.2 Precipitation

The precipitation anomalies for the El Niño composites for "POGA" in DJF and the following JJA and the differences between the other experiments and "POGA" are shown in figure 10. The most consistent and significant difference between the the experiments in DJF is over the Indian ocean. Here, reduced precipitation is seen in "POGA" but in the other experiments, the warm SSTAs imposed enhance the precipitation dramatically in the southwest Indian Ocean. The other experiments are also more similar to observed precipitation anomalies during El Niño (not shown). "POGA" also shows more enhanced equatorial precipitation over central and West Africa in DJF than the other experiments. The warm tropical Pacific and Indian Ocean SSTAs are therefore having a competing influence on central and West African precipitation in DJF which was also shown by Goddard and Graham (1999). However, HadAM3 has not been demonstrated to be accurate to this detail.

In JJA, after the event, the precipitation results have diverged further. "IPOGA", "TOGA" and "GOGA" have stronger drying in the eastern tropical Atlantic than "POGA". Therefore this drying is likely to be a consequence of Indian ocean warm SSTs as well as tropical Pacific warm SSTs. "POGA" has a large area of enhanced precipitation in the central Pacific, just north of the equator. This is damped out in "TOGA" and "GOGA". This is consistent with the sea level pressure results which suggest that the inclusion of the warm SSTAs in the tropical Atlantic serve to induce higher pressure over the tropical Pacific and hence descent and anomalous drying.

3.3 Upper Level Circulation

In order to study the processes by which the anomalies in one area influence the global circulation, anomalies of the 200hPa stream function of the non-divergent component of the flow and velocity potential of the divergent component are studied.

3.3.1 200hPa Velocity Potential

The anomalies of the 200hPa velocity potential of the divergent component of the flow for the El Niño composites in DJF and the following JJA are shown in figure 11. Differences between the experiments are not shown for velocity potential but all of the differences discussed are significant at the 98% confidence level. In DJF, all the experiments show the anomalous divergence above the enhanced precipitation over the warm El Niño SSTs of the central tropical Pacific. In "POGA", this is balanced by anomalous convergence above the Indian ocean and the north west Pacific. The zonal gradients of the velocity potential near the equator are associated with the Walker circulation and the meridional gradients with the divergent component of the Hadley circulation. The "POGA" results show a Walker circulation anomaly with convergence over the Indian ocean and divergence over the Pacific. The other three experiments have the descending branch of the anomalous Walker circulation more confined to the east of the Indian ocean and Maritime continent. This is closer to the observed response (not shown), again demonstrating the importance of the Indian ocean ENSO SSTAs for the tropics-wide response.

In JJA, after the event, "POGA" still has large scale anomalous divergence over the Pacific and convergence over the Indian ocean, although the meridional components have slackened. (The velocity potential being the divergence twice integrated.) In "POGA", the main tropical areas of anomalous convergence and divergence have changed little between DJF and JJA since the SST forcing consists of weak warm tropical Pacific SSTs and no remote forcing. However, in "IPOGA", the warm Indian ocean SSTs radically change the patterns of anomalous divergence. They suppress the upper level convergence over the Indian ocean and force convergence over the tropical Atlantic. Then for "TOGA" and "GOGA" in JJA, the tropics-wide warm SSTs mean the upper level circulation anomalies are globally weak - a result entirely different to both "POGA" and "IPOGA".

3.3.2 200hPa Stream Function

The anomalous 200hPa stream function for DJF and the following JJA of the El Niño composite for the "POGA" experiment are shown in figure 12. For the other experiments, the difference with "POGA" is plotted. The "POGA" DJF El Niño stream function shows the anomalous anticyclones straddling the equator above the warm SSTAs in the tropical Pacific, a well observed response to tropical heating (eg. Bjerknes, 1972). From

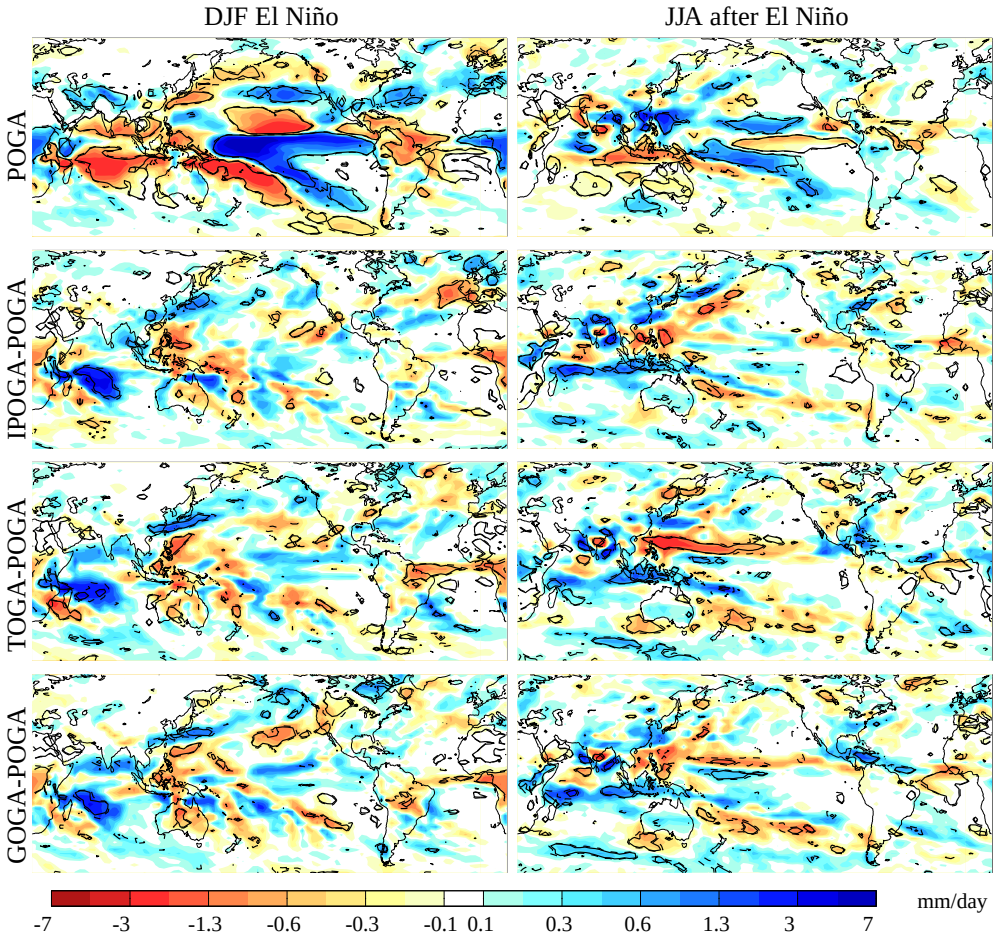

Figure 10: El Niño composite precipitation anomalies for "POGA" and differences from "POGA". Values significantly different from zero at the 98% and 95% confidence level are contoured with continuous and dashed contours respectively.

these anticyclones, Rossby wave trains emanate polewards and eastwards into the extratropics in both hemispheres as described by Hoskins and Karoly (1981). This propagation is stronger in the winter hemisphere as described by Trenberth et al. (1998). However, although this propagation into the extratropics displays some realistic behaviour, it is zonally misplaced by HadAM3 (Spencer and Slingo, 2003).

The other large remote response in DJF in "POGA" is above the Indian ocean. As with sea level pressure, the balance in the tropics of the tropical Pacific response, is to the west, above the Indian ocean with little response above the tropical Atlantic. When the warm Indian ocean SSTs are imposed in the other experiments, an additional anomalous anticyclonic couplet straddles the equator above the Indian ocean. This does not appear to be strong enough to force a significant extratropical response over Asia or south of the Indian ocean, unlike the erroneously strong response to Indian Ocean SSTAs reported by Kumar and Hoerling (1998). However, it does influence the atmosphere over the Atlantic in "IPOGA" in a manner similar to the forcing of the atmosphere above the Indian ocean by the Pacific in "POGA". This Atlantic response is damped in "TOGA" and "GOGA" once weak tropical Atlantic heating is imposed.

200hPa stream function anomalies are weak during JJA after El Niño for "POGA" consistent with the weak precipitation response seen in figure 10. There is a weak Rossby wave train arching into the southern extratropics (winter hemisphere) from the tropical Pacific in "POGA". The most consistent difference between "POGA" and the other experiments during JJA is over Australia and the south west Indian ocean, which is therefore likely to be forced by the warm Indian ocean and Maritime Continent SSTAs, part of the remote response to El Niño. Amongst others, Nicholls (1989) and Frederiksen and Balgovind (1994) have also shown the Indian ocean and Maritime Continent SSTAs to be influential on the Australian climate in JJA.

3.4 Surface Fluxes

Surface heat fluxes are thought to be the dominant mechanism by which ENSO atmospheric teleconnections create remote ENSO SSTAs (eg. Lau and Nath, 1996; Klein et al., 1999; Venzke et al., 2000). It has been shown that remote ENSO SSTAs are influential on the atmospheric teleconnections so it is important to be able to predict them. Therefore the net surface heat flux

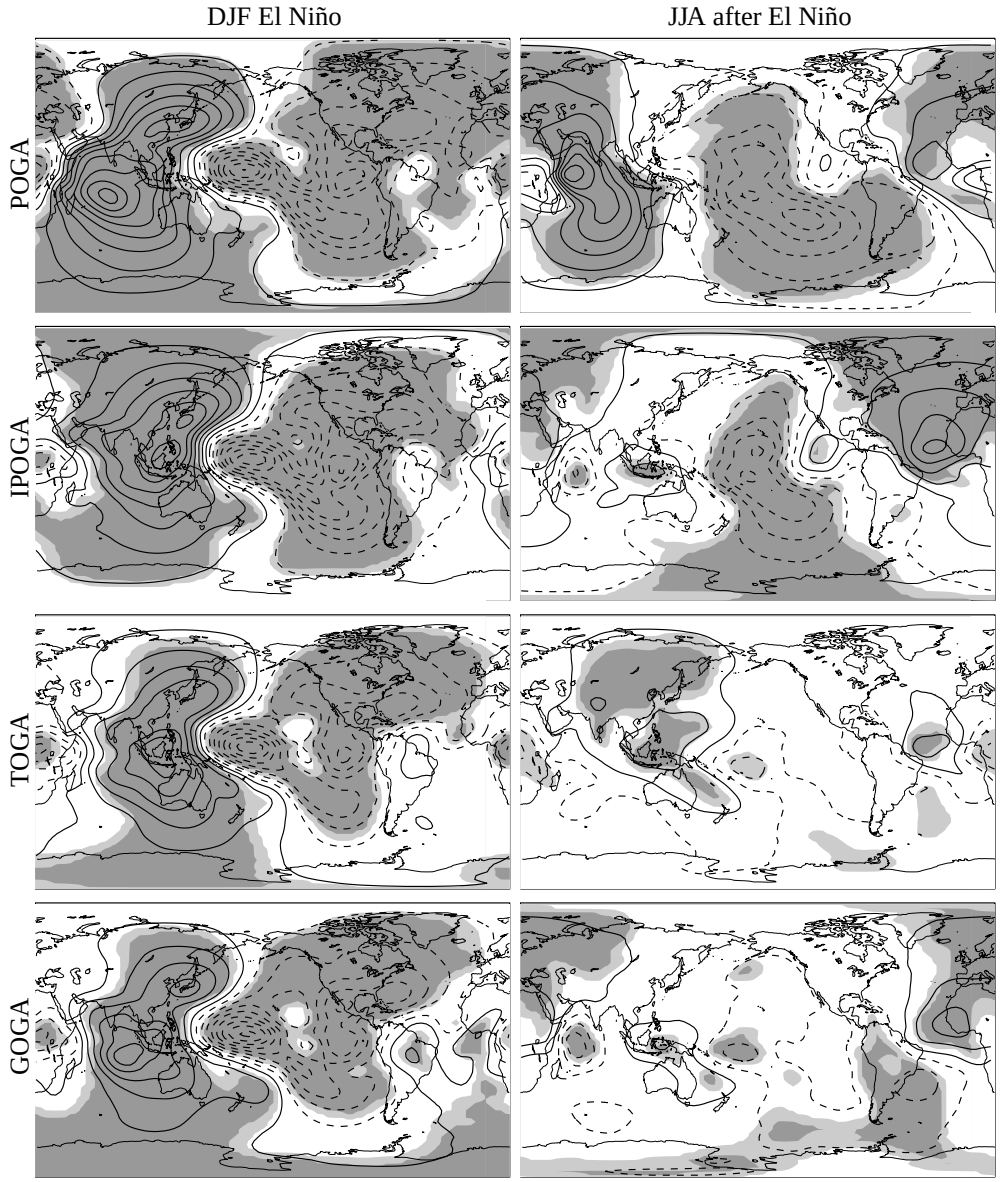

Figure 11: El Niño composite 200hPa velocity potential anomalies for the ENSO experiments. The contour interval is $0.5 \times 10^6 m^2 s^{-1}$, negative contours are dashed and start at $-0.25 \times 10^6 m^2 s^{-1}$. Values significantly different from zero at the 95% and 98% confidence levels are shaded light and dark respectively.

anomalies for each of the ENSO experiments are presented in order to study the predictability of the remote ENSO-related SSTAs.

The anomalous net downward surface heat flux during El Niño for "POGA" and differences with "POGA" for the other experiment are shown in figure 13. For this variable, values for SON before the peak of El Niño and DJF at the peak are plotted because heat flux anomalies take a few months to influence the SST significantly (eg. Pan and Oort, 1990; Klein et al., 1999; Venzke et al., 2000). As we are interested in the influences of remote ENSO SSTAs at and after the peak of ENSO, the heat flux anomalies before and at the peak are relevant. These heat fluxes include sensible and latent heat fluxes and solar and longwave radiation.

The "POGA" heat flux anomalies show a warming influence on the Indian Ocean during both seasons and in the tropical Atlantic during DJF. This agrees with the SSTAs observed during El Niño as shown in the composite in figure 3 and confirms the longer lag of the tropical Atlantic behind the Pacific than the Indian Ocean (eg Klein et al., 1999).

When the Indian Ocean ENSO SSTAs are additionally imposed in "IPOGA", the heat flux anomalies into the Indian Ocean are reduced. Also, positive heat flux anomalies are forced along the South Pacific convergence zone. However, apart from this aspect which is not studied further, the Indian Ocean SSTAs appear to have little impact on heat fluxes outside the Indian Ocean, unlike for the other atmospheric fields studied. This is likely to be partly because we are examining heat flux anomalies before and during the peak of ENSO rather than during and after the peak, when remote SSTAs become larger and more influential glob-

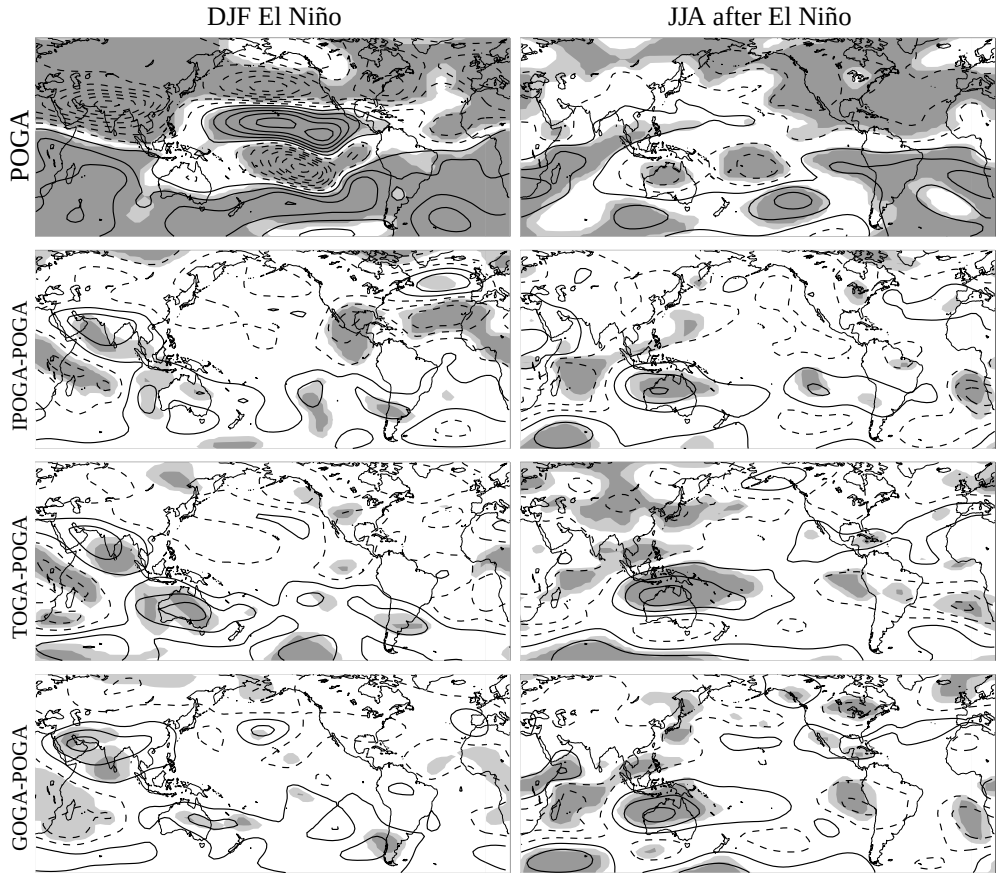

Figure 12: El Niño composite 200hPa stream function anomalies for the POGA experiments and differences with other experiments. The contour interval is $2 \times 10^6 m^2 s^{-1}$, negative contours are dashed and start at $-1 \times 10^6 m^2 s^{-1}$. Values significantly different from zero at the 95% and 98% confidence levels are shaded light and dark respectively.

ally. But also, in HadAM3, the processes influencing heat flux anomalies remotely, appear to be driven predominantly by the tropical Pacific SSTAs. This is a difference with sea level pressure and upper level circulation, which are significantly driven by each of the tropical oceans.

Similarly, the influence of the tropical Atlantic can be seen by comparing "IPOGA" and "TOGA" and these influences are small. The SSTAs imposed in the North Pacific in "GOGA" also damp the heat flux response as simulated in "TOGA".

These net surface heat flux results show that the remote tropical ENSO SSTAs observed during El Niño may be predictable by HadAM3. The local feedback from SST onto heat flux can be strong but the remote ENSO SSTAs do not strongly influence other heat fluxes up to the peak of El Niño.

4 Discussion and Conclusions

4.1 The Response to the West

The dominance of the atmospheric response to the west of tropical SSTAs was not entirely expected and requires some explanation. The Kelvin wave response to the east of equatorial heating, part of the Gill (1980) response, is manifest in the reduced precipitation in the Northeast of Brazil during DJF for "POGA" (figure 10). However, this direct Kelvin wave response is equatorially confined, limiting its geographical influence. The direct Rossby wave response, polewards and slightly westwards of the forcing, is also part of the Gill (1980) response and is most evident in the upper level anticyclones straddling the equator in the tropical Pacific shown in the 200hPa stream function anomalies for "POGA" in DJF (figure 12). The Gill (1980) response does not extend further westwards than this.

However, equatorial descent is also forced on the equator directly to the west of the anomalous ascent, over the Maritime Continent, manifest in the precipitation anomalies for "POGA" in DJF (figure 10). The anomalous descending Walker circulation branches to the west and east force anomalous Hadley circulations polewards, creating upper level cyclones straddling the equator, the opposite Rossby wave response. These are evident above the Indian Ocean, polewards and westwards of the equatorial anomalous descent but much weaker above the Atlantic as evident in the 200mb stream function anomalies in DJF for "POGA" (figure 12).

There are a number of possible reasons why this response in "POGA" above the Indian Ocean is so much bigger than that above the Atlantic. Firstly, the anomalous descent over the Maritime Continent is greater than

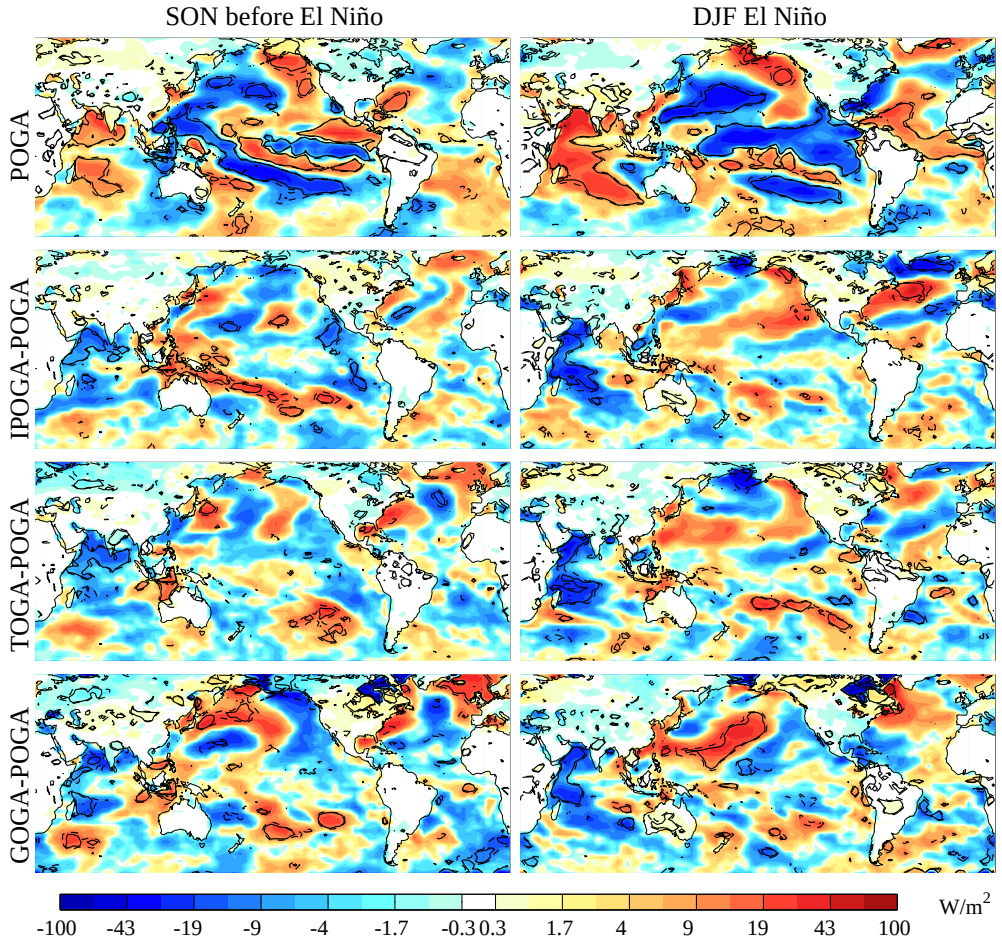

Figure 13: El Niño composite net surface heat flux anomalies into the ocean for the POGA experiments and differences with other experiments. Values significantly different from zero at the 95% and 98% confidence levels are contoured with dashed and continuous contours respectively.

that over the northeast of Brazil so the forcing of the Indian ocean is greater. Secondly, the anomalous descent over the Northeast of Brazil will have a Rossby wave response polewards and slightly westwards. This would overlap with the primary Pacific Rossby wave response of the upper level anticyclones and hence may not appear strongly. However, the Rossby wave response to the descent over the Maritime Continent would stretch westwards to above the Indian Ocean and therefore would not interfere with the primary tropical Pacific response.

A third possible reason for the response that appears to the west could be the meeting of the Rossby and Kelvin waves as described by Matthews (in press). In this study, convective anomalies over Africa during the northern summer monsoon were found to be related to the suppressed phase of the Madden-Julian Oscillation over the Maritime Continent 20 days earlier. Matthews (in press) shows that this anomalous suppressed convection over the Maritime Continent forces a westward propagating Rossby wave and an eastward propagating Kelvin wave which meet up 20 days later over Africa, favouring deep convection. The timescale for this adjustment is faster than the seasonal means studied here, but the location of the response that appears to be to the west is consistent with equatorial Rossby and Kelvin waves being forced over the central equatorial Pacific and meeting up over the Indian Ocean.

The results of these experiments and the possible explanations presented here are consistent with the results of Neale (1999), Hoskins et al. (1999) and Woolnough et al. (2001). Their studies included aquaplanet AGCM experiments with zonally symmetric SSTs, apart from localised SSTAs centred on the equator. Again, the response to the west was stronger than that to the east and extended further polewards and westwards. Hoskins et al. (1999) concluded that this Rossby wave response was not as simple as that described by Gill (1980). They attributed this to the distribution of heating in the vertical as well as the nonlinearity of the full AGCM. They also suggested that the Kelvin wave response to the east was weaker than that modelled by Gill (1980) because of the weaker and more realistic damping in a full AGCM.

4.2 The Influence of Remote ENSO SSTAs

This study has shown that remote ENSO SSTAs have an important role in determining the atmospheric component of the ENSO cycle: seasonal forecasts could be

improved and extended by taking these effects into account if they can be modelled sufficiently accurately. Leading up to the peak of an El Niño or La Niña event, most of the reproducible tropical atmospheric response is forced by the SSTs in the tropical Pacific since the remote ENSO SSTAs are small. However, through the peak and during the decay of the event, tropical Pacific SSTAs decay while remote ENSO SSTAs grow and become more influential. All of these model results have been found to be significant at the 98% confidence level based on a two-tailed t-test. In the context of seasonal prediction, forecast systems that can properly represent these ENSO-associated SSTAs and their impacts should have significantly enhanced skill compared to systems that neglect or misrepresent such effects.

In particular, the SSTAs of the Indian ocean and Maritime Continent are shown to be especially influential on the global response. This goes further than the results of Goddard and Graham (1999) who demonstrated the importance of the Indian ocean SST in simulating African rainfall and those of Nicholls (1989) and Frederiksen and Balgovind (1994) who showed how Australian winter rainfall is influenced by the Maritime Continent and Indian ocean SSTs. This study has shown the Indian ocean ENSO SSTAs to be influential not only on the immediate surroundings of the Indian Ocean but also on the entire Atlantic region. The Indian ocean is the second largest tropical ocean and its waters are already very warm so small changes in their temperature may lead to large atmospheric anomalies.

The tropical Atlantic ENSO SSTAs have been shown to damp the local atmospheric response and influence the atmosphere above the tropical Pacific after the peak of ENSO.

4.3 Final Conclusions

Finally, these experiments have helped to identify the reproducible response to ENSO SSTs in the tropical Pacific and the relative importance of the responses to remote ENSO SSTAs. The study of idealised ENSO cycles has shed light onto some of the teleconnection mechanisms. The removal of independent modes of ocean variability has enabled these experiments to show how the tropical Pacific influences the atmosphere above the Indian ocean but has less effect on the atmosphere above the tropical Atlantic. The subsequent Indian Ocean basin-wide warming associated with ENSO then damps the local response above the Indian Ocean and influences the atmosphere above the tropical Atlantic. Improved understanding of this delayed response to ENSO could lead to extended seasonal forecasts with atmospheric models which are coupled to the tropical oceans. It is through this coupling that the memory of the remote oceans after ENSO can be harnessed in order to improve seasonal forecasts. The Indian ocean has been shown to have significant influences on the tropics-wide climate which strengthens the argument for improved monitoring of this region. This would improve understanding of the nature of the coupling between the Indian and Pacific oceans and provide improved initial conditions for coupled models. The coupling between these two oceans and the influence of the Indian ocean on global climate is the subject of future research.

5 Acknowledgements

Some HadAM3 model results and the GISST sea surface temperature dataset were provided by the UK Met Office. H. Spencer and J. Slingo acknowledge support through the Natural Environment Research Council (NERC)-funded UK Universities' Global Atmospheric Modelling Programme and H. Spencer also received support from the Met Office through a CASE studentship. We are very grateful to Met Office staff who gave access to their data and to the CGAM tropical group who helped us to understand it. Thanks also to Lisa Goddard and two anonymous reviewers for comments on the manuscript.

References

Alexander M (1992) Midlatitude atmosphere-ocean interaction during El Niño. Part I: The North Pacific Ocean. J Clim.

Alexander M, Blade I, Newman M, Lanzante J, Lau N.-C, Scott J (2002) The atmospheric bridge: The influence of ENSO teleconnections on air-sea interaction over the global oceans. J Clim.

Barsugli J, Sardeshmukh P (2002) Global atmospheric sensitivity to tropical SST anomalies throughout the Indo-Pacific basin. J Clim.

Becker B, Slingo J, Ferranti L, Molteni F (2001) Seasonal predictability of the Indian summer monsoon: What role do land surface condotins play? MAUSAM, 52:175–190.

Bjerknes J (1972) Large-scale atmospheric response to the 1964-65 Pacific equatorial warming. J Phys Oceanogr, 2:212–217.

Brankovic C, Palmer T, Ferranti L (1994) Predictability of seasonal atmospheric variations. J Clim, 7:217–237.

Charney J, Shukla J (1981) Predictability of monsoons. In Lighthill J, Pearce R (eds) Monsoon Dynamics, Cambridge University Press, chapter 6.

Covey C, Abe-Ouchi A, Boer G, Boville B, Cubasch U, Fairhead L, Flato G, Gordon H, Guilyardi E, Jiang X, Johns T, Le Treut H, Madec G, Meehl G, Miller R, Noda A, Power S, Roeckner E, Russell G, Schneider E, Stouffer R, Terray L, von Storch J (2000) The seasonal cycle in coupled ocean-atmosphere general circulation models. Clim Dyn, 16:775–787.

Davey M, Huddleston M, Sperber K, Braconnot P, Bryan F, Chen D, Colman R, Cooper C, Cubasch U, Delecluse P, DeWitt D, Fairhead L, Flato G, Gordon C, Hogan T, Ji M, Kimoto M, Kitoh A, Knutson T, Latif M, Treut H. L, Li T, Manabe S, Mechoso C. R, Meehl G, Oberhuber J, Power S, Roeck-

ner E, Terray L, Vintzileos A, Voss R, Wang B, Washington W, Yoshikawa I, Yu J.-Y, Yukimoto S, Zebiak. S (2002) STOIC: a study of coupled model climatology and variability in tropical ocean regions. Clim Dyn, 18:403–420.

Fennessy M, Shukla L (1999) Impact of initial soil wetness on seasonal atmospheric prediction. J Clim, 12: 3167–3180.

Ferranti L, Molteni F, Palmer T (1994) Impact of localized tropical and extratropical SST anomalies in ensembles of seasonal GCM integrations. Q J R Meteorol Soc, 120:1613–1645.

Frederiksen C, Balgovind R (1994) The influence Of The Indian-Ocean Indonesian SST gradient on the Australian winter rainfall and circulation in an atmospheric GCM. Q J R Meteorol Soc, 120:923–952.

Gill A (1980) Some simple solutions for heat-induced tropical circulation. Q J R Meteorol Soc, 106:447–462.

Goddard L, Graham N (1999) Importance of the Indian Ocean for simulating rainfall anomalies over eastern and southern Africa. J Geophys Res, 104:19099–19116.

Graham R, Evans A, Mylne K, Harrison M, Robertson K (2000) An assessment of seasonal predictability using atmospheric general circulation models. Q J R Meteorol Soc, 126:2211–2240.

Gregory D, Rowntree P (1990) A mass flux convection scheme with representation of cloud ensemble charateristics and stability-dependent closure. Mon Weather Rev, 118:1483–1506.

Hoerling M. P, Hurrell J, Xu T (2001) Tropical origins for recent North Atlantic climate change. Science, 292:90–92.

Hoskins B, Karoly D (1981) The steady linear response of a spherical atmosphere to thermal and orographic forcing. J Atmos Sci, 38:1179–1196.

Hoskins B, Neale R, Rodwell M, Yang G (1999) Aspects of the large-scale tropical atmospheric circulation. Tellus Series A: Dynamical Meteorology and Oceanography, 51:33–44.

Kalnay E, Kanamitsu M, Kistler R, Collins W, Deaven D, Gandin L, Iredell M, Saha S, White G, Woollen J, Zhu Y, Leetmaa A, Reynolds B, Chelliah M, Ebisuzaki W, Higgins W, Janowiak J, Mo K, Ropelewski C, Wang J, Jenne R, Joseph D (1996) The NCEP/NCAR Reanalysis 40-year Project. Bull Am Meteorol Soc, 77:437–471. Web site http://www.cdc.noaa.gov.

Klein S, Soden B, Lau N (1999) Remote sea surface temperature variations during ENSO: Evidence for a tropical atmospheric bridge. J Clim, 12:917–932.

Koster R, Dirmeyer P, Hahmann A, Ijpelaar R, Tyahla L, Cox P, Suarez M, (2001) Comparing the degree of land-atmosphere interaction in four atmospheric general circulation models. J Hydrometeorol, 3:363–375.

Kumar A, Hoerling M (1998) Specification of regional sea surface temperatures in atmospheric general circulation model simulations. J Geophys Res, 103: 8901–8907.

Kumar A, Hoerling M, Leetma M, Sardeshmukh P (1996) Assessing a GCM's suitability for making seasonal predictions. J Clim, 9:115–129.

Latif M, Anderson D, Barnett T, Cane M, Kleeman R, Leetma A, O'Brien J, Rosati A, Schneider E (1998) A review of the predictability and prediction of ENSO. J Geophys Res, 103:14375–14313.

Latif M, Dommenget D, Dima M, Grötzner A (1999) The role of Indian Ocean sea surface temperature in forcing East African rainfall anomalies during December-January 1997/98. J Clim, 12:3497–3504.

Latif M, Sperber K, Arblaster J, Braconnot P, Chen D, Colman A, Cubasch U, Cooper C, Delecluse P, DeWitt D, Fairhead L, Flato G, Hogan T, Ji M, Kimoto M, Kitoh A, Knutson T, Le Treut H, Li T, Manabe S, Marti O, Mechoso C, Meehl G, Power S, Roeckner E, Sirven J, Terray L, Vintzileos A, Voss R, Wang B, Washington W, Yoshikawa I, Yu J, Zebiak S (2001) ENSIP: the El Niño simulation intercomparison project. Clim Dyn, 18:255–276.

Lau N.-C, Nath M (1994) A modelling study of the relative roles of tropical and extratropical SST anomalies in the variability of the global atmosphere-ocean system. J Clim, 7:1184–1207.

Lau N.-C, Nath M (1996) The Role of the "Atmospheric Bridge" in Linking Tropical Pacific ENSO Events to Extratropical SST Anomalies. J Clim, 9:2036–2057.

Matthews A (in press) Intraseasonal variability over tropical Africa during northern summer. J Clim.

Molteni F, Ferranti L. Non-linear aspects of the systematic errors of the ECMWF Coupled model. Technical report, ECMWF (2000).

Neale R. B. A study of the tropical response in an idealised global circulation model. Phd thesis, Meteorology, University of Reading, Earley Gate, PO Box 243, Reading, RG6 6BB, UK (1999).

Nicholls N (1989) Sea surface temperatures and Australian winter rainfall. J Clim, 2:965–973.

Pan Y, Oort A (1990) Correlation analyses between SST anomalies in the E. equatorial Pacific and the world Ocean. Clim Dyn, 4:191–205.

Parker D. E, Folland C. K, Jackson M (1995) Marine surface temperature: observed variations and data requirements. Climatic Change, 31:559–600.

Pope V, Gallani M, Rowntree P, Stratton R (2000) The impact of new physical parameterisations in the Hadley Centre climate model: HadAM3. Clim Dyn, 16:123–146.

Renshaw A, Rowell D, Folland C (1998) Wintertime low-frequency weather variability in the North Pacific-American sector 1949-93. J Clim, 11:1073–1091.

Sardeshmukh P, Compo G, Penland C (2000) Changes in probability associated with El Niño. J Clim, 13: 4268–4286.

Schneider E, Bengtsson L, Hu Z.-Z (2003) Forcing of northern hemisphere climate trends. J Atmos Sci, 60: 1504–1521.

Shukla J, Paolino D, Straus D, de Witt D, Fennessy M,

Kinter J, Marx L, Mo R, (2000) Dynamical seasonal predictions with the COLA atmospheric model. Q J R Meteorol Soc, 126:2265–2299.

Spencer H, Slingo J (2003) The simulation of peak and delayed ENSO teleconnections. J Clim, 16:1757–1774.

Taylor K. E (2001) Summarising multiple aspects of model performance in a single diagram. J Geophys Res, 106:7183–7192.

Trenberth K, Branstator G, Karoly D, Kumar A, Lau N.-C, Ropelewski C (1998) Progress during TOGA in understanding and modeling global teleconnections associated with tropical sea surface temperatures. J Geophys Res, 103:14,291–14,324.

Venzke S, Latif M, Villwock A (2000) The coupled GCM ECHO-2. Part II: Indian ocean response to ENSO. J Clim, 13:1371–1383.

Woolnough S, Slingo J, Hoskins B (2001) The organisation of tropical convection by intraseasonal sea surface temperature anomalies. Q J R Meteorol Soc, 127:887–907.